Anisotropic damage applied to numerical ductile rupture

Patrick Croix* — Franck Lauro* — Jérôme Oudin*
Jens Christlein**

* *Laboratory for Automation, Mechanical engineering, Information sciences and Human-machine systems, University of Valenciennes and Hainaut-Cambrésis, Valenciennes, France*
** *AUDI AG, Germany*

ABSTRACT. *Damage models models are applied for elasto-viscoplastic materials. They take microvoids volume fraction evolution into account by means of the growth, the nucleation and coalescence of microvoids. The anisotropy of the material is introduced with the Hill's potential in the modified yield function. The anisotropy of the damage is taken into account in one model with the shape of the microvoids. The void is defined as an ellipsoid which could evolve in shape and direction according to the loading direction and the geometry of the structure. These models are applied on unit cell specimens and on a double non-axisymmetrical V-notched specimen. The influence of the microvoids shape and their orientations on the final ductile rupture is shown.*

RÉSUMÉ. *Des modèles d'endommagement sont appliqués pour des matériaux élasto-viscoplastiques. L'évolution de la fraction volumique de vide est prise en compte par la croissance, nucléation et coalescence des microcavités. L'anisotropie du matériau est introduite par le potentiel de Hill dans la loi de relation de comportement modifié pour l'endommagement. L'anisotropie de l'endommagement est introduite dans un modèle par la prise en compte de la forme des cavités. Ces cavités sont définies comme ellipsoïdales et pouvant évoluer de forme et d'orientation selon la direction de chargement et la géométrie de la structure. Ces modèles sont utilisés pour des simulations d'essais de traction sur des éprouvettes simples et des éprouvettes entaillées en V de façon non axisymétrique. L'influence de la forme et de l'orientation des microcavités sur la description de la rupture ductile est montrée.*

KEYWORDS: *anisotropic damage, anisotropic behaviour, crack propagation.*

MOTS-CLÉS : *Anisotropie de l'endommagement, anisotropie de la loi de comportement, propagation de fissure.*

1. Introduction

Description of damage is required for numerical simulations of sheet metal forming processes, sheet metal stamping or vehicle crash tests in which internal deterioration plays a significant role.

Damage of porous material can be defined as a collection of permanent microstructural changes based on the description of the growth, nucleation and coalescence of the microvoids. This microscopic approach is described by several damage models which are applied to static loading (eg: extrusion, forging...) [BEN 93, 95] and dynamic loading (eg: crash, stamping...) [LAU 97, 98]. The Gurson's damage model [GUR 77], modified by Tvergaard and Needleman [TVE 81, 82, 84], is based on this damage process for isotropic materials. To introduce the anisotropy of the material, this damage model has been modified by introducing Hill's yield stress instead of the von Mises into Gurson-Tvergaard potential [DOE 95]. The microvoid shape, which is frequently expected to be at the origin of the anisotropic ductility, is taken into account in order to accurately predict an anisotropic damage. This model, based on the improved version of the Gologanu-Leblond-Devaux's model [GOL 93, 94, 97], extends the Gurson-Tvergaard's model to take the void shape effect into account. In order to emphasise the role of anisotropic void growth on ductile rupture, the microvoid shape is taken into account in its growth evolution. The description of the porous material is based on three internal variables: the microvoid volume fraction, shape and orientation. The microvoid volume fraction is defined as the ratio of the microvoid volume and the material volume. The microvoid shape corresponds to the difference between the Napierian logarithms of the minor and major semi axes of the microvoids and the orientation of microvoids changes with the rotation of the material. The sensitivity of the damage evolution is analysed in the case of prolate and spherical cavities with different loading directions. The anisotropy of the material is also introduced in the Gologanu-Leblond-Devaux model by means of the Hill 48 norm. Consequently some of the equations are modified. The new damage model for anisotropic microvoided material has been integrated into the three dimensional explicit finite element code for non-linear dynamic analysis of structures, PAM-SOLID^{TM}, in the case of convected coordinates shell elements. This paper will describe the constitutive damage model and its numerical implementation in the finite element code. The failure prediction is shown in the case of a non-axisymmetric double V-notched tensile specimen. Different anisotropic ductile ruptures are obtained according to the initial shapes of the cavities and their evolution.

2. Constitutive damage models

2.1. *Gurson's model*

The Gurson Tvergaard Needleman GTN model (1984) is a quadratic formulation of plastic potential which can also be used as a yield function as follows:

$$\phi_{evp} = \frac{\sigma_{eq}^2}{\sigma_M^2} - \varphi = 0 \qquad [1]$$

$$\text{where:} \quad \varphi = 1 + \left(q_1 f^*\right)^2 - 2 q_1 f^* \cosh\left(\upsilon\right), \qquad \upsilon = \frac{3}{2} q_2 \frac{\sigma_m}{\sigma_M} \qquad [2]$$

in which σ_{eq} is the macroscopic equivalent stress, σ_M is the elasto-viscoplastic flow stress, σ_m is the mean stress ($\sigma_m = \sigma_{kk} / 3$), q_1 and q_2 are the two "material" parameters introduced by Tvergaard [TVE 81] in order to converge the model with full numerical analyses of periodic arrays of voids. f^* is the Tvergaard and Needleman's coalescence function. The original GTN model used the von Mises norm: $\sigma_{eq}^2 = 1.5 \sigma'_{ij} \sigma'_{ij}$ where σ' is the macroscopic stress deviator. In this study it is replaced by the Hill 48 norm in order to take the anisotropic plastic behaviour into account[DOE 95], and in plane stress condition take the following form:

$$\sigma_{eq}^2 = \sigma_{11}^2 + \frac{F+H}{2} \sigma_{22}^2 - H \sigma_{11} \sigma_{22} + N \sigma_{12}^2 \qquad [3]$$

with F, H and N the Hill anisotropic parameters.

2.2. *Gologanu's model*

This is based on the studies of a material unit cell formed by two confocal spheroids. The Gologanu, Leblond and Devaux's model (GLD) extends the GTN model to take the microvoid shape effect into account, and is therefore interesting as it becomes the GTN potential for spherical microvoids.

The void shape is defined by the parameter $S = \ln\left(a_1 / b_1\right)$ where a_1 and b_1 are the major and minor axis of the ellipsoidal void. The GLD model is based on the analysis of an ellipsoidal cavity embedded in a medium Ω which has the shape of a confocal ellipsoid of minor and major semi-axes a_2 and b_2, the axis of the void is always collinear to the unit vector e_x (figure 1.). This cavity follows the rolling direction and is defined in the local frame of each element.

The plastic potential takes the following form:

$$\phi_{evp} = C\frac{\left\|\sigma' + \eta\sigma_H X\right\|^2}{\sigma_M^2} - \varphi = 0 \qquad [4]$$

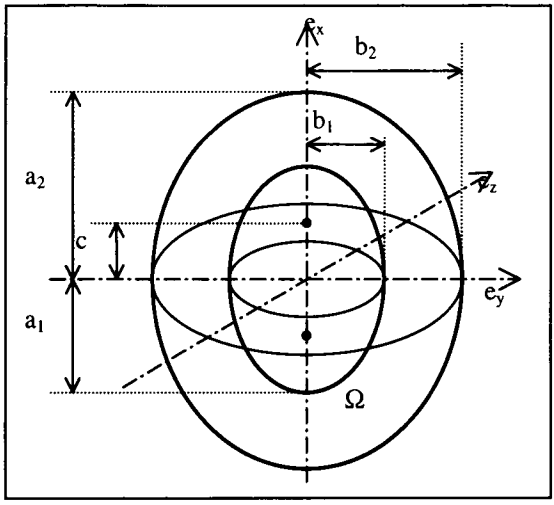

Figure 1. *The microstructureof a prolate cavity*

where:

$$\varphi = 1 + \left(q_1 f^*\right)^2 - 2q_1 f^* \cosh(\upsilon),\ \upsilon = \frac{\kappa\sigma_H}{\sigma_M},\ \sigma_H = (1-2\alpha_2)\sigma_{11} + \alpha_1\sigma_{22} \qquad [5]$$

The parameters κ, η, C and X are given by:

$$\kappa^{-1} = \frac{1}{\sqrt{3}} + \frac{1}{\ln(f)}\left[\left(\sqrt{3}-2\right)\ln\left(\frac{e_1}{e_2}\right) - \frac{1}{\sqrt{3}}\ln\left(\frac{3+e_1^2+2\sqrt{3+e_1^4}}{3+e_2^2+2\sqrt{3+e_2^4}}\right) + \ln\left(\frac{\sqrt{3}+\sqrt{3+e_1^4}}{\sqrt{3}+\sqrt{3+e_2^4}}\right)\right] \qquad [6]$$

$$\eta = -\frac{\kappa(1-f^2)sh}{1+f^2+f(\kappa H sh - 2ch)}$$
$$C = -\frac{\kappa f\, sh}{(1-f+\eta H)\eta},\quad sh \equiv \sinh(\kappa H),\quad ch \equiv \cosh(\kappa H),\quad H = 2(\alpha_1 - \alpha_2) \qquad [7]$$

$X = \frac{1}{3}\left(2e_x \otimes e_x - e_y \otimes e_y - e_z \otimes e_z\right)$, with e_x, e_y, e_z the axis of the frame of the void and where the eccentricities e_1, e_2 and the parameter α_2 are deduced from the void shape parameter S and the void volume fraction f by the following equations:

$$e_1 = \sqrt{1 - e^{-2|S|}} \qquad [8]$$

$$\frac{e_2^3}{1 - e_2^2} = f \frac{e_1^3}{1 - e_1^2} \qquad [9]$$

$$\alpha_2 = \frac{1 + e_2^2}{3 + e_2^4} \qquad [10]$$

The notation $\| \bullet \|$ is used in the original GLD potential to express the calculation of the von Mises norm $\left(\|T_{ij}\| = \left[1.5\, T_{ij} T_{ij}\right]^2 \right)$ applied to the deviator stress σ' on which $\eta \sigma_H X$ is added. In this paper the material anisotropy is introduced with the Hill 48 norm and then a transformation of the deviatoric expression $\sigma' + \eta \sigma_H X$ is required.

Moreover, considering plane stress strate , and assuming the microvoid direction e_x follows the rolling direction, the deviatoric stress tensor $\sigma' + \eta \sigma_H X$ is expressed as:

$$\sigma' + \eta \sigma_H X = \frac{1}{3} \begin{bmatrix} 2a\sigma_{11} + (-1+2b)\sigma_{22} & 3\sigma_{12} & 0 \\ 3\sigma_{12} & -a\sigma_{11} + (2-b)\sigma_{22} & 0 \\ 0 & 0 & -a\sigma_{11} - (1+b)\sigma_{22} \end{bmatrix}$$

with $a = 1 + \eta(1 - 2\alpha_2)$ and $b = \eta \alpha_2$.

Then the Hill 48 norm presented for Gurson's model is modified and expressed as follows:

$$\sigma_{eq} = \left[a^2 \sigma_{11}^2 + \left(b^2 + \frac{H+F}{2} - Hb \right) \sigma_{22}^2 + (2ab - Ha)\sigma_{11}\sigma_{22} + N\sigma_{12}^2 \right]^{1/2} \qquad [11]$$

For the particular case of spherical voids (S = 0) the parameter κ and α_2 are respectively equal to 3/2 and 1/3 and the GLD model is identical to GTN model.

This model is completed by the equation of the evolution of the internal shape parameter S given by:

$$\dot{S} = \frac{3}{2} \left(1 + \frac{9}{2} h_T(T,\zeta) \left(1 - \sqrt{f}\right)^2 \frac{\alpha_1 - \alpha_1^G}{1 - 3\alpha_1} \right) \left(\dot{\varepsilon}_{11} - \frac{\dot{\varepsilon}_{kk}}{3} \right) + \left(\frac{1 - 3\alpha_1}{f} + 3\alpha_2 - 1 \right) \dot{\varepsilon}_{kk} \qquad [12]$$

with $h_T(T,\zeta)$ a function, dependent on the triaxiality $T \equiv \sigma_{kk} / (3\sigma_{eq})$ according to the sign of $\zeta = \sigma_{kk} \sigma'_{ii}$, given by:

$$\begin{cases} h_T(T,\zeta) = 1 - T^2 & \text{for } \zeta > 0 \\ h_T(T,\zeta) = 1 - \dfrac{T^2}{2} & \text{for } \zeta < 0 \end{cases} \quad [13]$$

and α_1 and α_1^G are obtained by:

$$\alpha_1 = \frac{1}{2e_1^2} - \frac{1-e_1^2}{2e_1^3}\tanh^{-1}(e_1) \quad [14]$$

$$\alpha_1^G = \frac{1}{3-e_1^2} \quad [15]$$

The evolution of the micro structural damage is represented by the current void volume fraction f, defined by $f = 1\text{-}V_M/V_A$, where V_A, V_M are respectively the elementary apparent volume of the material and the corresponding volume of the matrix.

f^* is a function of the void volume fraction f

$$f^* = \begin{cases} f & \text{if } f \le f_c \\ f_c + \dfrac{1/q_1 - f_c}{f_F - f_c}(f - f_c) & \text{if } f > f_c \end{cases} \quad [16]$$

where f_c is the critical microvoid volume fraction at coalescence onset, f_F is the microvoid volume fraction when ductile fracture occurs. This specific function f^* inside the microvoid material potential describes the rapid loss of the stress carrying capacity due to the coalescence of the neighbouring microvoids, when f reaches the limit $1/q_1$.

The microvoids volume fraction evolution has two main phases: the nucleation of the new voids and the growth of existing voids. The microvoids volume fraction rate is expressed by:

$$\dot{f} = \dot{f}_{\text{growth}} + \dot{f}_{\text{nucleation}} \quad [17]$$

The constitution from void nucleation is controlled by plastic strain [CHU 80], and takes the form:

$$\dot{f}_{\text{nucleation}} = \frac{f_N}{S_N\sqrt{2\pi}}\exp\left\{-\frac{1}{2}\left(\frac{\varepsilon_M - \varepsilon_N}{S_N}\right)^2\right\}\dot{\varepsilon}_M = A_1\dot{\varepsilon}_M \quad [18]$$

where f_N is the nucleated microvoid volume fraction, S_N is the Gaussian standard deviation, ε_N is the mean effective plastic strain for nucleation and ε_M is the effective plastic strain.

The growth of existing voids is given by:

$$\dot{f}_{growth} = (1-f)\dot{\varepsilon}_{kk} \qquad [19]$$

the equivalence between the plastic work dissipated into the porous material and the ductile matrix is expressed as follows:

$$(1-f)\sigma_M \dot{\varepsilon}_{kk} = \sigma : D^p$$

which leads to the following expression of the effective plastic strain rate

$$\dot{\varepsilon}_M = \frac{\sigma : D^p}{(1-f)\sigma_M} \qquad [20]$$

in which σ is the Cauchy stress tensor, σ_M is the elasto-viscoplastic flow stress and D^p is the macroscopic plastic strain rate tensor defined in the case of the associated plasticity by:

$$D^p = \dot{\lambda}\frac{\partial \phi_{evp}}{\partial \sigma} \qquad [21]$$

The plastic multiplier $\dot{\lambda}$ is deduced from the consistency condition $\phi_{evp} = 0$ and $\dot{\phi}_{evp} = 0$ leading to solve:

$$\phi_{evp} = \dot{\phi}_{evp} = \frac{\partial \phi_{evp}}{\partial \sigma} : \dot{\sigma} + \frac{\partial \phi_{evp}}{\partial \sigma_M} : \dot{\sigma}_M + \frac{\partial \phi_{evp}}{\partial f} : \dot{f} = 0 \qquad [22]$$

The plastic multiplier is finally expressed by

$$\dot{\lambda} = \frac{\phi_{evp}}{\frac{\partial \phi_{evp}}{\partial \sigma} : C^e : \frac{\partial \phi_{evp}}{\partial \sigma} - \frac{\partial \phi_{evp}}{\partial \sigma_M}\frac{\partial \sigma_M}{\partial \varepsilon_M} A_2 - \frac{\partial \phi_{evp}}{\partial f}\left[(1-f)\frac{\partial \phi_{evp}}{\partial \sigma} : I + A_3\right]} \qquad [23]$$

$$\text{with } A_2 = \frac{\sigma : \frac{\partial \phi_{evp}}{\partial \sigma}}{(1-f)\sigma_M} \qquad [24]$$

$$\text{and } A_3 = A_1 \cdot A_2 \qquad [25]$$

where C^e is the isotropic material tensor and I is the second order identity tensor.

2.3. *Numerical Implementation*

The previous constitutive damage model is implemented in the finite element code PAM-SOLID™.

This code uses an explicit process in which the solution is advanced along the time axis, along which the velocities are discretised at half time intervals, ${}^{n-1/2}t$, ${}^{n+1/2}t$... and the displacements and accelerations are discretised at full time intervals, ${}^{n-1}t$, ${}^{n}t$, ${}^{n+1}t$... where n is the number of the time increment. Considering a given time ${}^{n}t$, the program calculates from the known quantities, which are the nodal velocity ${}^{n-1/2}V$ the nodal displacement ${}^{n}X$ and the Cauchy stress ${}^{n-1}\sigma$; the updated or unknown quantities ${}^{n}\sigma$, ${}^{n+1/2}V$, ${}^{n+1}X$, ${}^{n}a$ the nodal acceleration and F_{int}, F_{ext}, the internal and external nodal forces, respectively. The new development consists of the stress calculation described below (Figure 2.).

Assuming the strain rate tensor ${}^{n-1/2}\dot{\varepsilon}_{ij}$ computed at the previous time increment as elastic, the corresponding Cauchy stress tensor is updated by central finite difference

$$ {}^{n}\sigma_{ij} = {}^{n-1}\sigma_{ij} + \left({}^{n}t - {}^{n-1}t\right)^{n-1/2} C^{e}\,\dot{\varepsilon}_{ij} $$

in which ${}^{n}\sigma_{ij}$ depends on ${}^{n}\sigma_{xx}$, ${}^{n}\sigma_{yy}$, ${}^{n}\sigma_{xy}$ in the case of shell elements.

The corresponding potentials are obtained by $\phi_{evp} = \sqrt{C}\,{}^{n}\sigma_{eq} - {}^{n-1}\sigma_{M}\sqrt{\varphi} = 0$ then all the derivation comes from this equation.

3. Numerical examples

3.1. *Unit cells tensile test*

In order to study the anisotropic damage evolution several unit cell tensile tests containing ellipsoidal void shapes are carried out. Two loading directions L and T are considered which are respectively along the major and minor axis of the voids.

To take only the anisotropic effect of the void shape into account, the isotropic von Mises criterion is considered and for this the G, F, N Hill's parameter are respectively equal to 1, 1 and 3 in this study.

Tests with the GTN model and the GLD model are performed on a unit cell model with an initial spherical void. Two tests are performed on a unit cell model with an initial prolate void according to the loading directions L and T to exhibit the anisotropic damage evolution.

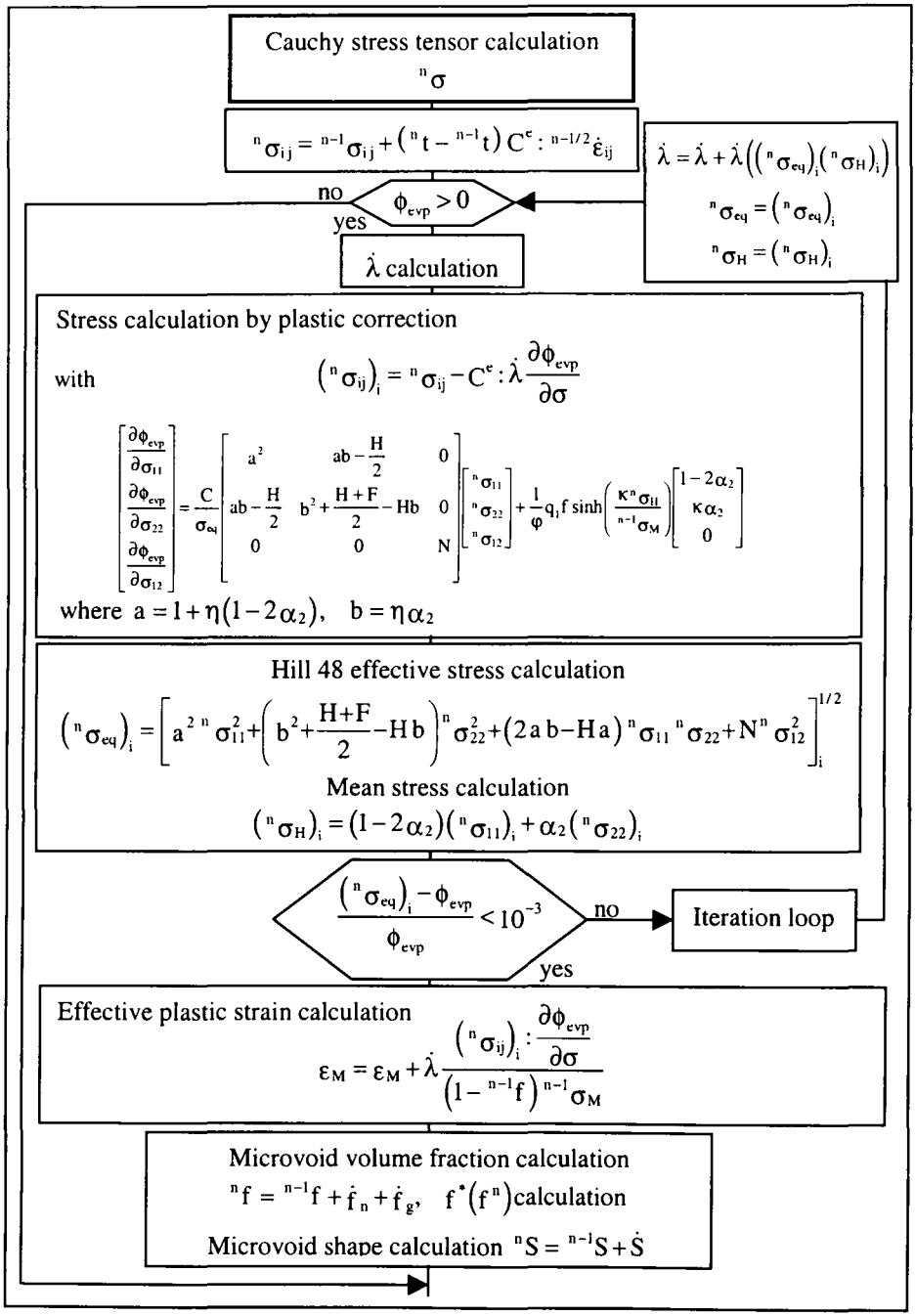

Figure 2. *The modified stress elastic prediction and plastic correction flowchart*

E_t (MPa)	65 000	647	600	450	300.5
σ_M (MPa)	195	206	218	227	518

Table 1. *Flow stress*

This analysis carried out with a standard elastoplastic material; the flow stress is described by successive tangent moduli (Table1)

The usual material parameters are, q_1=1.5, q_2=1. for the elasto-viscoplastic potential, f_0=10^{-4} for the initial void volume fraction, f_N=0.04, S_N=0.1 and ε_N=0.2 for the nucleation and the coalescence is not considered with f_C = 1. f_F = 1. These parameters are obtained from literature [TVE 82], [NEE 85, 87].

The damage evolution of these tensile tests based on the plastic strain is presented in figure 3.

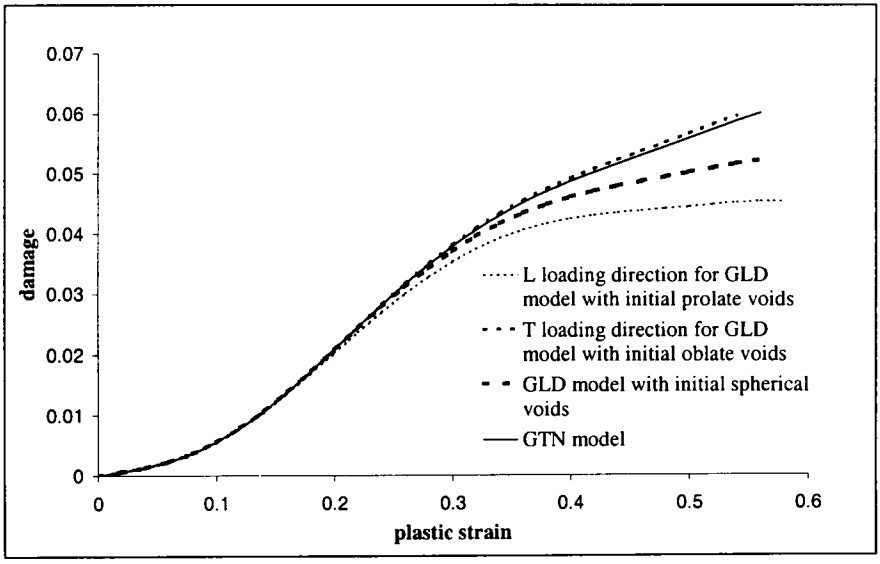

Figure 3. *Damage evolution based on the plastic strain for the tensile tests*

The GTN model could be considered as the reference but it's generally well known that it overestimates the damage in the structure. It is directly compared to the GLD model with initial spherical voids.

The GTN model has spherical voids which stay spherical during the deformation. With the GLD model the initial spherical voids become ellipsoidal in the direction of the deformation and consequently the damage evolution is more difficult and increases slower than with the GTN model, as seen in figure 3.

Consequently, the damage value is more realistic. In the case of prolate voids, the damage value is greater for the loading direction T than for the loading direction L (figure 3.).

It is really due to the combination of the shape of the voids and the loading direction. For the direction L, the prolate voids tend to become more and more prolate with an increase of the parameter S which corresponds to the ratio between the major and minor axis of the ellipse. For the direction T, on the contrary, the prolate voids tend to become oblate voids with an inversion of the ratio between the major and minor axis of the ellipse. The parameter S then evolves to S positive to S negative. Consequently, the area of the voids for this case is greater than with the loading direction L and the evolution of the parameter S is quicker and leads to more damage and of course to a quicker rupture (figures 3 and 4).

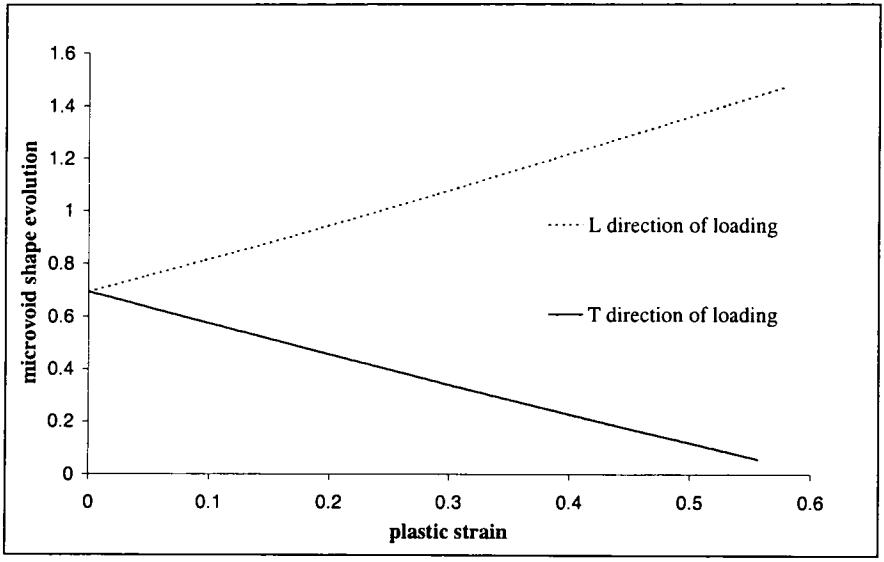

Figure 4. *Shape evolution according longitudinal and transverse loading directions*

3.2. *Non axisymmetrical double V-notched specimen*

The aim of the numerical simulation is to confirm that the GLD model is more accurate in predicting crack propagation than the GTN model. Thus, the numerical description of crack propagation for a non-axisymmetric double V-notched tensile test specimen is performed using both the GTN and GLD models. This crack propagation is obtained by elimination of successive elements which occurs at the complete loss of the stress carrying capacity. To avoid numerical divergence the stress in the element is put to zero when it reaches the damage value $f = 0.9\ f_F$. The figure 6a. presents the initial mesh size.

The porous elasto-viscoplastic material is described as the previous material for the unit cell tensile test. The values of the material parameters are the result of an industrial requirement and are obtained with using an inverse method [LAU 99]. This method consists in the identification of the damage parameters by correlating an experimental and numerical macroscopic measurement strongly dependent on the parameters. The macroscopic measurement is given by means of a tensile test on a notched specimen. It corresponds to the variation of the inner radius of the specimen in function of the elongation. In order to take the anisotropic aspect of the microvoid shape parameter S into account, three experimental measurements are considered. They correspond to three tensile tests specimen at 0°, 45° and 90° with the rolling direction. An optimiser is used to find the damage parameters minimising the gap between numerical and experimental measurements in all the directions at the same time. Due to the symmetry of the specimen, one quarter of its finite element model is used and the result for only one direction (0°) is presented in figure 5. This identification process is applied for Gurson's parameters as well as Gologanu's parameters.

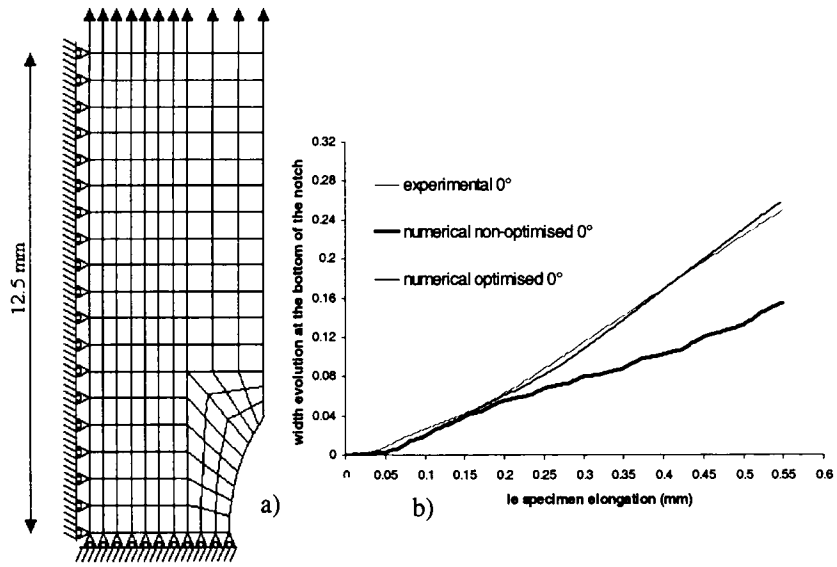

Figure 5. *a) Finite element modelling, boundary conditions for one quarter of the notched tensile specimen. b) Comparison of experimental-numerical width evolution at the bottom of the notch according to the tensile specimen elongation, for a specimen sample along the rolling direction*

The material has an anisotropic behaviour which is introduced by Hill's parameters G, F and N.The initial void shape used with the GLD model is prolate with S = ln(4) = 1.3863.

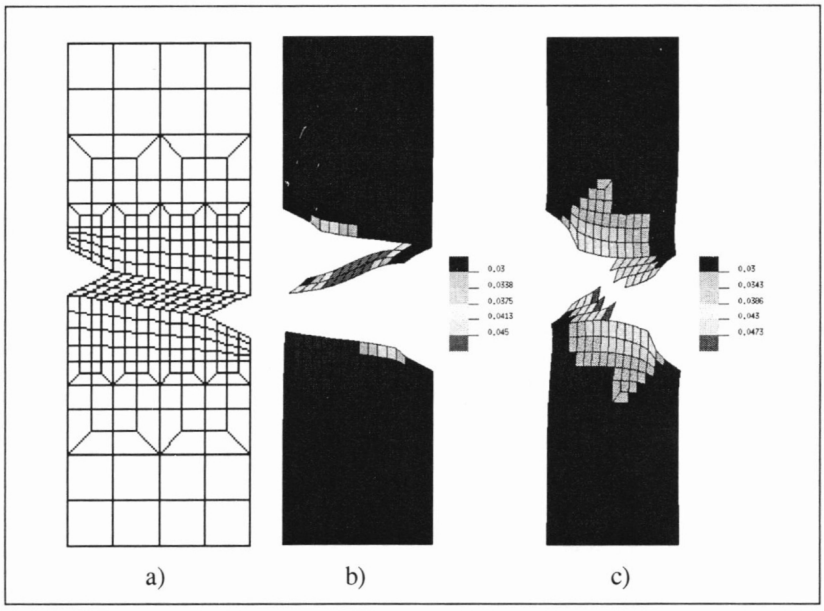

Figure 6. *Tensile test of a non-axisymmetrical double V-notched specimen, a) initial finite element modelling; b) and c) are the damage distribution at the end of the process using the GTN and GLD models respectively*

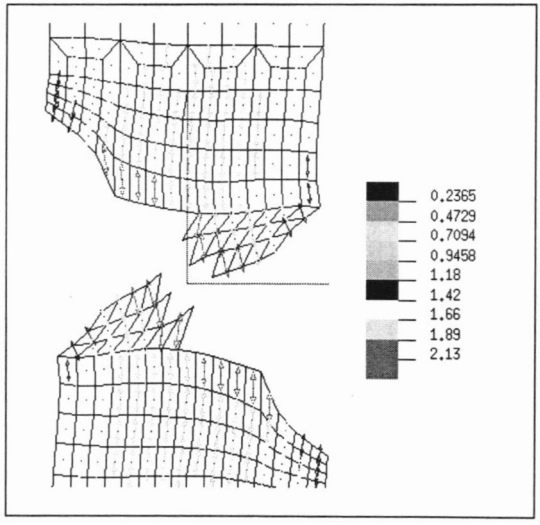

Figure 7. *Tensile test of a non-axisymmetrical double V-notched specimen, orientation and shape evolution S at the end of the process for an initial prolate void shape using the GLD model*

Figures 6b. and 6c. show the results from the computations after rupture with the GTN model and the GLD model, respectively. The GTN model shows that cracks are initiated at the bottom of the notches and propagated in opposite directions without ever coming into contact. The result with the GLD model differs from that obtained with the GTN model. The rupture initiation is identical for both models but with the GLD model the cracks tend to meet each other and the final rupture occurs in the middle of the test specimen which is the experimental result. This difference is due to the shape of the voids and their orientations. Due to the shape of the specimen, the main plastic strain direction is different in the middle of the V-notches. Consequently, the voids rotate to follow the main axis of deformation and this leads to a better estimation of the crack propagation. The orientation of voids is described by vectors and presented in figure 7. The length of these vectors is proportional to the shape parameter value.

4. Conclusion

The GTN and GLD models are used to predict the damage evolution occurring with plastic strain. Both models are based on the description of the porosity of the material by the microvoid volume fraction and the prediction of the porous material flow by a modified yield surface. The evolution of the microvoid volume fraction due to the growth of existing microvoids and the nucleation of new microvoids is taken into account. The ductile rupture is finally predicted. These models have been modified by introducing the Hill's potential into the elasto-plastic potential to take the anisotropy of the material into account. Moreover, the GLD model defines different initial shape of voids (prolate, spherical, and oblate) which change of shape, and orientation during the deformation.

First of all the two damage models are presented in this paper. The implementation of the GLD model in the explicit finite element code PAM-SOLID™ is then explained in more detail. Two different elementary tests are presented. First of all, a unit cell computation highlights the effect of the shape of the voids on the damage evolution and moment of rupture. These tests illustrate that:

– the damage evolution is better predicted with the GLD model than the GTN model which generally overestimates the damage;

– in the case of prolate voids, the damage evolution differs if the loading direction corresponds to the direction of the major axis or the minor axis of the ellipse.

Secondly, tensile tests of non-axisymmetrical V-notched specimens are performed with the GTN and GLD models. These tests show that the direction of the propagation of the crack is better predicted with the GLD model due to the change of orientation of the voids according to the direction of the main plastic strain during deformation. Finally, two different ruptures are obtained with the GTN and GLD models and the GLD model gives closer results to the experimental ones.

5. References

[BEN 93] BENNANI B., PICART P., OUDIN J., « Some basic finite element analysis of microvoid nucleation, growth and coalescence », *Engineering Computations*, vol. 10, 1993, p. 409-421.

[BEN 95] BENNANI B., OUDIN J., « Backward can extrusion of steels effects of punch design on flow mode and void volume fraction », *International Journal of Machine Tools and Manufacture*, vol. 35, 1995, p. 903-911.

[CHU 80] CHU C., NEEDLEMAN A., « Void nucleation effects in biaxially stretched sheets », *Journal of Engineering Materials and Technology*, vol. 102, 1980, p. 249-256.

[DOE 95] DOEGE E., EL-DSOKI T., SEIBERT D., « Prediction in necking and wrinkling in sheet-metal forming », *Journal of Materials Processing Technology*, vol. 50, 1995, p. 197-206.

[GOL 93] GOLOGANU M., LEBLOND J.B., DEVAUX J., « Approximate models for ductile metals containing non-spherical voids—Case of Axisymmetric prolate ellipsoidal cavities », *Journal of the mechanics and physics of solids*, vol. 41, 1993, p. 1723-1754.

[GOL 94] GOLOGANU M., LEBLOND J.B., DEVAUX J., « Numerical and theoretical Study of coalescence of cavities in periodically Voided solids », *Computational Material Modelling*, vol. 42, 1994, p. 223-244.

[GOL 97] GOLOGANU M., LEBLOND J.B., PERRIN G., DEVAUX J., « Recent's extensions of Gurson model for porous ductile metals », *Continuum micromechanics*, 1997, P. Suquet ed., New York.

[GUR 77] GURSON A. L., « Continuum theory of ductile rupture by void nucleation and growth: Part I —Yield criteria and flow rules for porous ductile media », *Engineering Material Technology*, vol. 99, 1977, p. 2-15.

[LAU 97] LAURO F., BENNANI B., DRAZETIC P., OUDIN J., NI X., « Damage occurrence under dynamic loading for strain rate sensitive materials », *Communications in Numerical Methods in Engineering*, vol. 13, 1997, p. 113-126.

[LAU 98] LAURO F., BENNANI B., OUDIN J., NI X., « Damage occurrence under dynamic loading for anisotropic strain rate sensitive materials », *Shock and Vibration*, vol. 5, 1998, p. 43-51.

[LAU 99] LAURO F., BENNANI B., CROIX P., OUDIN J., « Identification of the damage parameters for anisotropic materials by inverse technique: application to an aluminium », *Proceedings of the International Conference on Advances in Materials and Processing Technologies, AMPT'99*, Dublin, 3-6 August 1999, Editors Profs. M.S.J. Hashmi, and Dr L. Looney.

[NEE 85] NEEDLEMAN A., TVERGAARD V., « Material strain rate sensitivity in round tensile bar », *Proc. Considère Mem. Symp., Salençon J. Ed., Presse de l'école Nationale des Ponts et Chaussées*, 1985, p. 251-262.

[NEE 87] NEEDLEMAN A., « A continuum model for void nucleation by inclusion debonding », *Journal of Applied Mechanics*, vol. 54, 1987, p. 525-531.

[TVE 81] TVERGAARD V., « Influence of voids on shear band instabilities under plane strain conditions », *International Journal of fracture*, vol. 17, 1981, p. 389-407.

[TVE 82] TVERGAARD V., « On localization in ductile materials containing spherical voids », *International Journal of fracture*, vol. 18, 1982, p. 237-252.

[TVE 84] TVERGAARD V., NEEDLEMAN A., « Analysis of the cup-cone fracture in around tensile bar », *Acta Metallurgica*, vol. 32, 1984, p. 157-169.